EXPERIMENTAL DEMONSTRATION OF ADVANTAGE OF MOTION INDUCED SYNTHETIC APERTURE RADIOMETER

Hyuk Park, Sung-Hyun Kim, Ho-Jin Lee, Nam-Won Moon, Hwan-Wook Yu, Up Namgoong, Won-Seon Sim, and Yong-Hoon Kim*

Gwangju Institute of Science and Technology (GIST), yhkim@gist.ac.kr

ABSTRACT . Aperture synthesis with platform motion has been presented as a useful tool to achieve the high spatial resolution imaging. Using a motion induced synthetic aperture radiometer (MISAR), a passive microwave image can be achieved with a small number of antennas. Moreover, the MISAR is capable of imaging better than the case without motion, using the same configuration of antenna array. With a platform motion, visibility can be sampled more efficiently, and as a result the imaging performance of the MISAR shows higher quality than the case without platform motion. In this paper, the advantage of MISAR is demonstrated experimentally. Using a laboratory model of inteferometric radiometer, the point source images are obtained under the condition with platform motion and without platform motion. In the experimental results, the point source response of the MISAR shows better quality of sidelobe level and beam efficiency than the case without platform motion.

KEY WORDS: Passive microwave remote sensing, Aperture synthesis, Radiometry

1. INTRODUCTION

A poor spatial resolution is a main problem in passive microwave remote sensing. In order to obtain useful spatial resolution on an airborne or spaceborne platform, a very large size of aperture is necessary, but it is very difficult when using a real aperture antenna in microwave band. The aperture synthesis technique has provided a practical solution to this problem. Instead of using a large real antenna, a large aperture can be synthesized using an antenna array consisting of many small antennas. On the past few decades, many studies have been conducted on this synthetic aperture radiometer (Ruf et al., 1988) and (Kerr et al. 2001).

Meanwhile some different types of synthetic aperture radiometer have been proposed. The synthetic aperture radiometer has not considered basically the platform motion, but some have proposed the aperture synthesis with the platform motion (Komiyama, 1991), (Edelsohn, 1992), (Camps and Swift, 2001), and (Park and Kim, 2008). This type of radiometer can be called Motion Induced Synthetic Aperture Radiometer (hereafter MISAR). It has been reported that a large aperture can be synthesized more efficiently using the platform motion compared with the case without motion. In other words, if the platform motion is accompanied in aperture synthesis, the same size of aperture can be generated with less number of antennas. The MISAR, therefore, can employ a sparse array which cannot show the acceptable performance in the aperture synthesis without the platform motion.

In this paper, the advantage of the MISAR is demonstrated by experiment. First we explain the advantage of the MISAR in more detail, and discuss the experimental procedure and the results.

2. ADVANTAGE OF THE MISAR

The main advantage of the MISAR is that a large aperture can be synthesized with less number of antennas compared with the radiometer without the platform motion. It results from more efficient coverage of the spatial frequency of the MISAR. In this section, the advantage of the MISAR is discussed on the basis of the spatial frequency coverage (often referred to as (u,v) coverage). Before turning into the detail discussion, it should be noted that the MISAR scenario and notation of parameters are followed by those in (Park and Kim, 2008). More detailed explanation of the observation can be found in (Park and Kim, 2008), including the meaning of the parameters.

2.1 Spatial Frequency Coverage of the MISAR

In aperture synthesis, (u,v) coverage affects deeply the imaging performance. For example, a synthesized beam width, sidelobe levels are largely affected by how well the antenna array samples the spatial frequencies. The analysis of (u,v) coverage, therefore, will provide a clue as to why the MISAR imaging is more efficient than the aperture synthesis without the platform motion.

The spatial frequencies u and v are given by an antenna spacing divided by wavelength, D_{kl} / λ, in the case without the platform motion. However, it should be formulated by a different form for the MISAR because the phase term in the visibility function depends on time t and the position of source (x_o, y_o) as well as the antenna spacing D_{kl}. For the aperture synthesis with motion, the instantaneous spatial frequency is given by

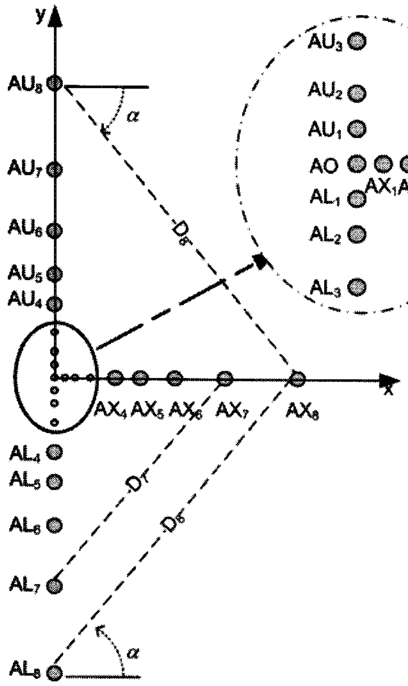

Figure 1. Antenna array configuration of the sparse T-shaped array for the experiment.

$$u_{kl}(t;x_o,y_o) = \frac{D_{kl}\sqrt{y_o^2+H_0^2}}{\lambda}\frac{\left[v_a t y_o \sin\alpha - \left(y_o^2+H_0^2\right)\cos\alpha\right]}{\left(v_a^2t^2+y_o^2+H_0^2\right)^{3/2}} \quad (1)$$

$$v_{kl}(t;x_o,y_o) = \frac{D_{kl}\sqrt{y_o^2+H_0^2}}{\lambda}\frac{\left[-v_a t y_o \cos\alpha - \left(v_a^2t^2+H_0^2\right)\sin\alpha\right]}{\left(v_a^2t^2+y_o^2+H_0^2\right)^{3/2}} \quad (2)$$

where all meaning of parameters in (1) and (2) are described in (Park and Kim, 2008). As shown in (1) and (2), the (u,v) coverage of the MISAR is not the same as D_{kl}/λ, and it leads the advantage of the MISAR by efficient with (u,v) coverage. It is shown more clearly in the next section with an example of the MISAR scenario.

2.2 Example of Spatial Frequency Coverage of the MISAR

Here, an example of the MISAR scenario is introduced for the convenience of discussion. A T-shaped array configuration for the MISAR is shown in Figure 1. It has the twenty times of wavelength for the largest baseline, that is, $D_8 = 20\lambda$. More details of array configuration are explained in (Park and Kim, 2008). The other parameters are as follows; platform height $H_0 = 800$ km, antenna tilt angle to the across-track $\bar{\theta} = 45°$,

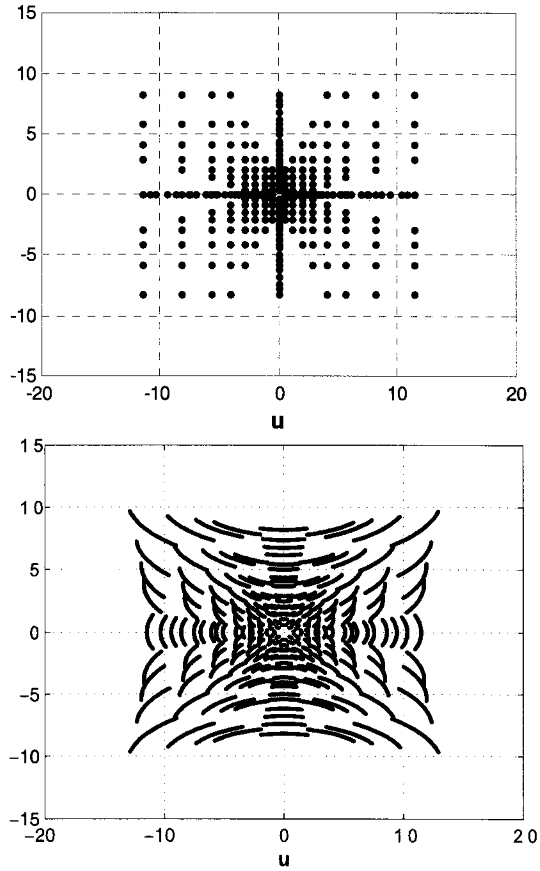

Figure 2. Spatial frequency coverage for the example scenario: the aperture synthesis without platform motion (upper), and the MISAR (lower).

elementary antenna half power beamwidth (HPBW) $BW_x = 20°$ to along-track and $BW_y = 30°$ to across-track, corresponding footprint $2L_x = 960$ km and swath width $2L_y = 1000$ km, receiver center frequency $f_0 = 1.4$ GHz, and noise bandwidth $B = 20$ MHz. The platform observes the brightness source at $(x_o, y_o) = (0, 800)$ km from $-x_i = -480$ km $(= -L_x)$ to $-x_i = -480$ km $(= +L_x)$.

Figure 2 shows the spatial frequency coverage of the case study; the upper is for the scenario without platform motion, and the lower is for the scenario with the platform motion. As shown in Figure 2, the spatial frequencies of the radiometer without motion covers (or are sampled) on the point. On the other hand, the MISAR samples the spatial frequencies over the line. Consequently, when using the same array configuration, the MISAR covers the spatial frequency more densely than the case without platform motion. This merit results in the better imaging performance such as the sidelobe levels, and the beam efficiency. It will be demonstrated in the next section with the experimental results.

Table 1. RF specification of the two-channel correlation radiometer for the experiment.

Parameter	Receiver 1 and 2
Center Frequency	37 GHz
Bandwidth	2 GHz
Output frequency	1.95 GHz
Local oscillator frequency	38.95 GHz
Local oscillator power	7 dBm
Gain	30 dBm
Noise figure	3.8 dB

3. EXPERIMENT AND RESULTS

3.1 Laboratory Model Radiometer for Experiment

It is very difficult to implement the actual MISAR system and observation on the platforms such as satellites and flights. The experiment therefore was performed with a laboratory model, Two-channel Ka-band correlation radiometer (Choi, 2003). Actually, the MISAR system requires the number of receiver as much as the number of antennas.

The two-channel (single baseline) correlation radiometer was exploited for the experiment because the implementation of the whole receiver channel is difficult. As changing the relative position of antennas, we have composed the T-shaped array configuration virtually. The block-diagram of the receiver and the RF specification are listed in Table 1. For the data acquisition and sampling, Tektronix oscilloscope is used. In the MISAR system, the delay lines are inserted before cross-correlation of the signals of two channels. The delay process (phase compensation) was performed by software. In other words, the signal was time-shifted by amount of pre-calculated delay after signal acquisition and storage, and then cross-correlated.

3.2 Experiment procedure

As shown in Figure 3 (a), a noise point source was located on an EM (electromagnetic) absorber background as an imaging target. To minimize the external effect, the noise source with high brightness temperature was used, which consists of a matched load, two amplifiers, and a patch antenna. After installing the point source, we located the receiving antennas on the metal plate as shown in Figure 3 (c).

The metal plate has holes where the T-shaped array configured shown in Figure 1. The metal plate was fixed on the long frame bar which guides the path of the platform. Then, the point source signal is received with two-channel correlation radiometer and stored. After storing, the metal plate was moved to right by predetermined distance (2 cm in the experiment), and fixed on the frame-bar again. As repeating this process from the leftmost to the rightmost of the frame-bar, the MISAR observation of single baseline was conducted on the laboratory. After one baseline measurements obtained,

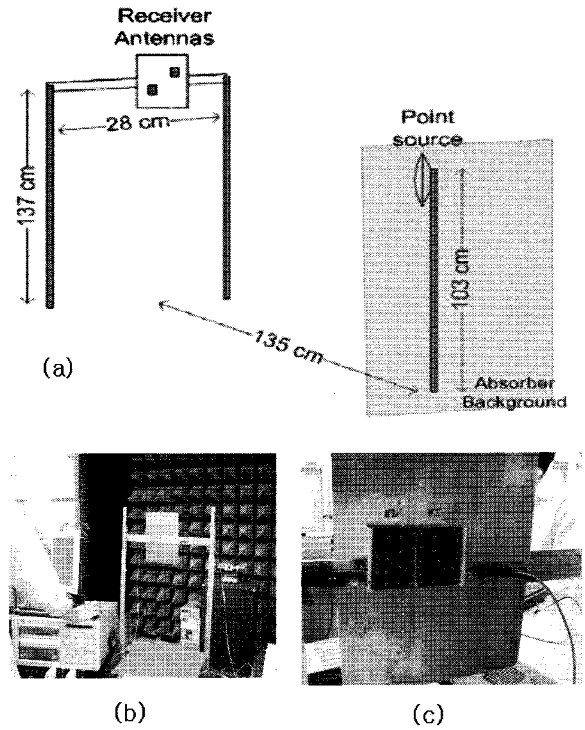

Figure 3. Experimental setup: (a) conceptual diagram, (b) picture of the actual experiment, and (c) the plate for the antenna installation.

the antenna position was changed on the metal plate to form another baseline. The experiment were performed for measure the MISAR point source imaging by repeating the one baseline measurement again, and changing the antenna position to cover the whole baseline configuration of the T-shaped array.

On the experiment, the observation parameters are as follows: Height $H_0 = 135$ cm, source incidence angle $\theta_i = 15°$, observation angel $12°$, and spatial sampling rate $2\,\text{cm}$.

3.3 Experimental results

After measuring the brightness source signal using radiometer, the point source responses are reconstructed for two cases: the case without the platform motion, and the MISAR. The different thing in the experiment from what was discussed before is that the experiment uses the S/W delay lines instead of H/W delay lines. Using the data acquisition and storage, the experimental system directly stores the brightness source signal received by two channels without delay lines and cross-correlation. Then, the delay compensation and cross-correlation are executed by S/W.

The aperture synthesis without the platform motion uses the measurement at a certain x position (along track); it does not consider the platform moving. Hence, the platform is assumed to be stay on $x = 0$, and the image is reconstructed with the measurements on that position.

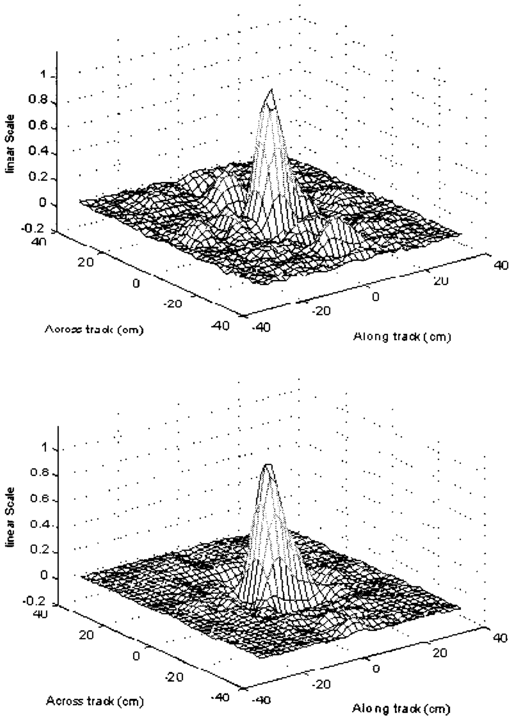

Figure 4. Experimental results for the point source response: aperture synthesis without the platform motion (upper) and the MISAR scenario (lower).

Table 2. Performances for the experimental points source response.

Performances criteria	No motion	MISAR
-3 dB pixel size (along track)	4.5 cm	4.5 cm
-3 dB pixel size (across track)	5 cm	5 cm
beam efficiency at -3 dB	0.21	0.31
beam efficiency at -10 dB	0.51	0.59
sidelobe level (along track)	-9 dB	-9 dB
sidelobe level (across track)	-6 dB	-9 dB

Figure 4 shows the point source response of the experiment; the upper is the point source response of the aperture synthesis without platform motion, and the lower is from the MISAR scenario. The performances of each response are listed in Table 2.

The experimental results reveal the advantage of the proposed MISAR system well. Compared with the case without the motion, Figure 4 upper image, the point source response of the MISAR, Figure 4 lower image, shows better imaging performance in sidelobe and beam efficiency. The experimental results reflect the (u, v) coverage of two systems. The (u, v) coverage of the case without the motion is too sparse so that the point source response shows high sidelobe and low beam efficiency. On the other hand, the (u, v) coverage of the MISAR is relatively dense so that the point source response shows better performance than the other case. Therefore, it is demonstrated that the MISAR image is more efficient that the aperture synthesis without the platform motion.

4. CONCLUSION

The MISAR system as an aperture synthesis with platform motion has an advantage compared with the case without the platform motion. It is capable of covering the spatial frequency more densely than the other case, with the same configuration of antenna array. Therefore, the MISAR shows better imaging performance such as low sidelobes, and better beam efficiency. In this research, this advantage of the MISAR has been demonstrated by the laboratory experiment. Using the Ka-band two channel correlation radiometer, the points source responses were obtained under the MISAR scenario and the case without motion. In the experimental results, the MISAR shows better results than the other case; the sidelobe level and the beam efficiency are better in the point source response of the MISAR. Through the study, we conclude that the MISAR imaging is more efficient than the aperture synthesis without the platform motion.

ACKNOWLEDGEMENTS (OPTIONAL)

This work was supported by (KICOS) through a grant provided by the Korean Ministry of Education, Science Technology (MEST) in K20701010357-07B0100-10710.

REFERENCES

Ruf, C., C. Swift, A. Tanner, and D. LeVine, 1988, Interferometric synthetic aperture microwave radiometry for the remote sensing of the earth, IEEE Trans. Geosci. Remote Sensing, 26(5), pp. 597-611.

Kerr, Y., P. Waldteufel, J. P. Wigneron, J. Martinuzzi, J. Font, and M. Berger, 2001, Soil moisture retrieval from space: the soil moisture and ocean salinity (smos) mission. IEEE Trans. Geosci. Remote Sensing, 39(8), pp. 1729–1735.

Komiyama, K., 1991, High resolution imaging by supersynthesis radiometers (ssr) for the passive microwave remote sensing of the earth. *Electron. Lett.*, 27(1), pp. 389-390.

Edelsohn, C., 1992, Synthetic array radiometry. *Proc. International Geoscience and Remote Sensing Symposium, IGARSS '92*, 2, pp. 1429-1431.

Camps, A., and C. Swift, 2001, A two-dimensional doppler-radiometer for earth observation. *IEEE Trans. Geosci. Remote Sensing*, 39(7), pp. 1566-1572.

Park, H., and Y.-H. Kim, 2008, Improvement of the Doppler-Radiometer Using a Sparse Array. *IEEE Geosci. Remote Sensing Letters*, accepted.

Choi, J.-H, 2003, A study on design of Ka-band interferometric synthetic aperture radiometer receiver, *Ph. D. Dissertation, Gwangju Institute of Science and Technology.*